Available online at www.sciencedirect.com

ScienceDirect

journal homepage: www.jfda-online.com

Review Article

Reactive oxygen species-related activities of nano-iron metal and nano-iron oxides☆

Haohao Wu [a,b,c], Jun-Jie Yin [c,*], Wayne G. Wamer [c], Mingyong Zeng [a], Y. Martin Lo [b]

[a] College of Food Science and Engineering, Ocean University of China, 5 Yushan Road, Qingdao, Shandong Province 266003, China
[b] Department of Nutrition and Food Science, University of Maryland, College Park, MD 20742, USA
[c] Center for Food Safety and Applied Nutrition, US Food and Drug Administration, College Park, MD 20740, USA

ARTICLE INFO

Article history:
Received 30 September 2013
Received in revised form
19 December 2013
Accepted 21 December 2013
Available online 5 February 2014

Keywords:
Iron oxide
Metallic iron
Nanoparticle
Reactive oxygen species
Toxicity

ABSTRACT

Nano-iron metal and nano-iron oxides are among the most widely used engineered and naturally occurring nanostructures, and the increasing incidence of biological exposure to these nanostructures has raised concerns about their biotoxicity. Reactive oxygen species (ROS)-induced oxidative stress is one of the most accepted toxic mechanisms and, in the past decades, considerable efforts have been made to investigate the ROS-related activities of iron nanostructures. In this review, we summarize activities of nano-iron metal and nano-iron oxides in ROS-related redox processes, addressing in detail the known homogeneous and heterogeneous redox mechanisms involved in these processes, intrinsic ROS-related properties of iron nanostructures (chemical composition, particle size, and crystalline phase), and ROS-related bio-microenvironmental factors, including physiological pH and buffers, biogenic reducing agents, and other organic substances.

1. Introduction

Reactive oxygen species (ROS), resulting from the transfer of energy or electrons to oxygen, are highly reactive and potentially harmful to living organisms [1]. These ROS, such as singlet oxygen, superoxide, hydrogen peroxide, and hydroxyl radical, are essential intermediates in certain physiological processes (e.g., photosynthesis, respiration, and cell signaling), and their levels within cells are tightly controlled via enzymes (e.g., superoxide dismutase, glutathione peroxidase, and catalase) or antioxidants (e.g., ascorbic acid, cysteine, glutathione, bilirubin, carotenoids, and bilirubin). However, this redox homeostasis can be perturbed in many circumstances, and a burst of ROS, a condition termed oxidative stress, can induce deleterious effects to cells through oxidative damage of biomolecules (e.g., proteins,

☆ The views presented in this paper are those of the authors and do not necessarily reflect official positions or policies of the US Food and Drug Administration.

* *Corresponding author*. Center for Food Safety and Applied Nutrition, US Food and Drug Administration, College Park, MD 20740, USA. E-mail address: junjie.yin@fda.hhs.gov (J.-J. Yin).

http://dx.doi.org/10.1016/j.jfda.2014.01.007

lipids, and nucleic acids) or disruption in cell signaling mechanisms [2].

Advances in nanotechnology, which deals with materials with dimensions of the order of 100 nm or less, have resulted in increasing commercial applications of engineered nanoparticles in consumer products, such as electronics, medicines, dietary supplements, food, clothing, cosmetics, and goods for children. The use of nanomaterials in diverse categories of consumer products suggests that broad populations of consumers will be increasingly exposed to nanomaterials [3,4]. A large number of studies have been conducted to evaluate the biological effects of nanoparticle exposure, and ROS-induced oxidative stress has been well recognized as one of the most important mechanisms when toxicity is observed [5].

Iron, which plays an active redox-catalytic role in many energy-transfer or electron-transfer processes due to its partially filled d orbitals and variable oxidation states, is inextricably linked to ROS chemistry. Engineered nanostructures of iron, including nano-iron metal and nano-iron oxides, have attracted commercial interest in areas of medicine (e.g., intravenous iron preparations, iron supplements, magnetic resonance imaging contrasting agents, drug and gene delivery, tissue engineering, and hyperthermia), food (e.g., iron fortificants), environment (e.g., remediation of soils and water by removal of organic pollutant and heavy metals), and agriculture (e.g., plant fertilizer and animal feed). Therefore, understanding ROS-related activities of nano-iron metal and nano-iron oxides could help address concerns over increasing incidences of biological exposure to these engineered nanostructures [6–11]. There are also widespread naturally-occurring iron nanostructures in diverse parts of terrestrial and aquatic ecosystems (e.g., soils, sediments, rivers, lakes, springs, and marine) mainly in the form of iron oxides, including ferrihydrite ($FeHO_8{\cdot}4H_2O$), lepidocrocite (γ-FeOOH), goethite (α-FeOOH), hematite (α-Fe_2O_3), maghemite (γ-Fe_2O_3), and magnetite (Fe_3O_4), thus making ROS-related activities of nano-iron oxides critical in comprehending ecological roles of naturally-occurring iron nanostructures [12].

This review focuses on activities of nano-iron metal and nano-iron oxides in ROS-related redox processes. The known redox mechanisms involved in these processes are demonstrated first, followed by a description of intrinsic ROS-related properties of iron nanostructures. Finally, ROS-related bio-microenvironmental factors are also discussed.

2. ROS-related redox mechanisms of nano-iron metal and nano-iron oxides

Successive one-electron or two-electron reduction of molecular oxygen to water in the aqueous solution yields a series of ROS such as superoxide radicals ($O_2^{\cdot-}/HO_2^{\bullet}$), hydrogen peroxide ($H_2O_2$), and hydroxyl radicals ($OH^{\bullet}$). Nano-iron metal and nano-iron oxides can be involved in these redox reactions as the reactant or catalyst via a homogeneous or heterogeneous means, based on dissolved iron species or solid surfaces, respectively. The standard reduction potentials (E^0) of redox pairs covered in this review are cited from previous studies [13–15].

2.1. *Homogeneous reactions*

(1) The classic homogeneous Fenton reaction, which involves one-electron reduction of hydrogen peroxide by soluble ferrous iron species, generates hydroxyl radicals ($E^0 = +2.3$ V) that are powerful enough to oxidize most organic molecules:

$$Fe(II) + H_2O_2 \rightarrow Fe(III) + OH^- + {}^{\cdot}OH \quad (1)$$

By convention, Fe(II) and Fe(III) represent all ferrous and ferric iron species, respectively.

(2) The non-radical mechanism for the homogeneous Fenton reaction involves the generation of ferryl-oxo complexes ($E^0 = +0.9$ V), less powerful oxidants compared to hydroxyl radicals, via two-electron reduction of hydrogen peroxide with soluble ferrous iron species:

$$Fe(II) + H_2O_2 \rightarrow Fe(IV)O^{2+} + H_2O \quad (2)$$

Based on the distinct oxidizing power of hydroxyl radicals and ferryl-oxo complexes, many studies have found that radical and non-radical Fenton reactions are competing reactions with a pH-dependent partitioning [16–18].

(3) The homogeneous Fenton-like reactions, which involve the generation of superoxide radicals, hydroxyl radicals, or ferryl-oxo complexes from hydrogen peroxide and soluble ferric iron species, consist of two steps; a slow one-electron reduction of ferric iron by hydrogen peroxide and a rapid generation of powerful oxidants via reaction (1) or (2):

$$Fe(III) + H_2O_2 \rightarrow Fe(II) + HO_2^{\cdot}/O_2^{\cdot-} + H^+ \quad (3)$$

$$Fe(II) + H_2O_2 \rightarrow Fe(III) + OH^- + {}^{\cdot}OH, \quad (1)$$

$$Fe(II) + H_2O_2 \rightarrow Fe(IV)O^{2+} + H_2O \quad (2)$$

(3) The Haber-Weiss reaction, which involves generation of hydroxyl radicals from hydrogen peroxide and superoxide, can be catalyzed by soluble ferric iron species through two steps:

$$Fe(III) + HO_2^{\cdot}/O_2^{\cdot-} \rightarrow Fe(II) + H_2O/OH^- + O_2 \quad (4)$$

$$Fe(II) + H_2O_2 \rightarrow Fe(III) + OH^- + {}^{\cdot}OH \quad (1)$$

(4) The homogeneous Fe(II) autoxidation in the presence of molecular oxygen in the aqueous solution via single-step two-electron transfer or stepwise one-electron transfer reactions can generate oxidants of ferryl-oxo complexes or a series of ROS [19,20]:

$$Fe(II) + O_2 \rightarrow Fe(IV)O^{2+} \quad (5)$$

$$Fe(II) + O_2 \rightarrow Fe(III) + HO_2^{\cdot}/O_2^{\cdot-} \quad (6)$$

$$Fe(II) + HO_2^{\cdot}/O_2^{\cdot-} \rightarrow Fe(III) + H_2O_2 \quad (7)$$

$$Fe(II) + H_2O_2 \rightarrow Fe(III) + OH^- + {}^{\cdot}OH \quad (1)$$

$$Fe(II) + H_2O_2 \rightarrow Fe(IV)O^{2+} + H_2O \quad (2)$$

(5) The homogeneous auto-scavenging reactions involving evolution of molecular oxygen and oxidative loss of soluble ferrous iron species [21]:

$$H_2O_2 + {}^{\cdot}OH \rightarrow HO_2^{\cdot}/O_2^{-\cdot} + H_2O \quad (8)$$

$$HO_2^{\cdot}/O_2^{-\cdot} + HO_2^{\cdot}/O_2^{-\cdot} \rightarrow H_2O_2 + O_2 \quad (9)$$

$$Fe(II) + {}^{\cdot}OH \rightarrow Fe(III) + OH^- \quad (10)$$

$$Fe(IV)O^{2+} + Fe(II) + H^+ \rightarrow 2Fe(III) + OH^- \quad (11)$$

2.2. *Heterogeneous reactions*

It has long been recognized that iron oxides can initiate heterogeneous redox reactions at the aqueous-solid interface. Zalma et al [22] reported that iron oxides including akaganeite, magnetite, crocidolite, and hematite were active in producing hydroxyl radicals in the presence of hydrogen peroxide by redox reactions initiated at the solid surface. Lin and Gurol [23] found that the kinetic model of catalytic decomposition of hydrogen peroxide by the granular goethite in aqueous solution at pH 7 was similar to the classical Langmuir-Hinshelwood rate model, which usually describes heterogeneous surface reactions, and proposed a redox mechanism of iron oxides based on the surface-complexation chemistry of surface-bound ferric [≡Fe(III)] and ferrous [≡Fe(II)] iron:

$$\equiv Fe(III) + H_2O_2 \rightarrow \equiv Fe(II) + HO_2^{\cdot}/O_2^{-\cdot} + H^+ \quad (12)$$

$$\equiv Fe(II) + H_2O_2 \rightarrow \equiv Fe(III) + OH^- + {}^{\cdot}OH \quad (13)$$

$$\equiv Fe(III) + HO_2^{\cdot}/O_2^{-\cdot} \rightarrow \equiv Fe(II) + H_2O/OH^- + O_2 \quad (14)$$

Non-radical surface initiated redox mechanisms were also reported by Watts et al [24] and Pham et al [25]:

$$\equiv Fe(III) + H_2O_2 \rightarrow \equiv Fe(II) + +HO_2^{\cdot}/O_2^{-\cdot} + H^+ \quad (12)$$

$$\equiv Fe(II) + H_2O_2 \rightarrow \equiv Fe(IV) + 2OH^- \quad (15)$$

In 2013, Fang et al [26] proposed that magnetite nanoparticles could heterogeneously catalyze the generation of hydrogen peroxide from dissolved molecular oxygen in the aqueous solution via the superoxide intermediate:

$$\equiv Fe(II) + O_{2(aq)} \rightarrow \equiv Fe(III) + HO_2^{\cdot}/O_2^{-\cdot} \quad (16)$$

$$\equiv Fe(II) + HO_2^{\cdot}/O_2^{-\cdot} \rightarrow \equiv Fe(III) + H_2O_2 \quad (17)$$

Metallic or zero-valent iron, which is a two-electron donor through the redox pair of Fe^{2+}/Fe^0 with an E^0 of −0.44 V, can directly reduce dissolved molecular oxygen in aqueous solutions to hydrogen peroxide at its solid surface according to the well-studied iron corrosion theory:

$$Fe^0_{(s)} + O_{2(aq)} \rightarrow Fe(II) + H_2O_2 \quad (18)$$

Hydrogen peroxide added exogenously or produced by reaction (18) can also heterogeneously oxidize zero-valent iron into ferrous iron:

$$Fe^0_{(S)} + H_2O_{2(aq)} \rightarrow Fe(II) + 2OH^- \quad (19)$$

Disassociated or surface-bound ferrous iron heterogeneously produced by reaction (18) or reaction (19) could then react with hydrogen peroxide or molecular oxygen via homogeneous reactions of (1), (2), (5), (6), and (7), or heterogeneous reactions of (13), (15), (16), and (17), to generate oxidants of hydroxyl radicals or ferryl-oxo complexes [27].

3. Intrinsic ROS-related properties of iron nanostructures

3.1. *Chemical composition*

According to reactions (5), (6), and (16), iron nanostructures containing Fe^0 and Fe(II) could directly reduce molecular oxygen dissolved in the aqueous solution to generate ROS or ferryl-oxo complexes through a homogeneous or heterogeneous mechanism, whereas pure ferric oxides have not been reported to react with aqueous dissolved molecular oxygen. According to Xue et al [28], higher ratios of structural Fe(II) seem to favor the heterogeneous redox reactivity of iron (II, III) oxides toward hydrogen peroxide decomposition and ROS production at neutral pH [28]. Gorski et al [29] also revealed that magnetite with a higher ratio of Fe(II) had a lower E^0 and a higher redox reactivity. Voinov et al [30] demonstrated that the magnetite nanoparticles were significantly more effective in producing hydroxyl radicals than the maghemite nanoparticles at the same ratio of the nanoparticle total surface and reaction volume. According to Chen et al. [31], magnetite nanoparticles also exhibited a higher catalytic efficiency in both hydrogen peroxide decomposition and hydroxyl radical production [31].

3.2. *Particle size*

Particle size can affect both homogeneous and heterogeneous redox reactions of iron nanostructures, and the underlying mechanisms involve the size-dependent features such as surface area and surface physicochemical properties. Homogeneous redox reactions of iron nanostructures depend on the concentrations of dissolved iron species, which originate from a heterogeneous process (i.e., iron dissolution) so heterogeneous reactions are prerequisite for both redox mechanisms. The rate of a heterogeneous process is usually a function of surface area, which increases rapidly with decreasing particle size, and this has also been verified in redox reactions of iron nanostructures. As Sponza and Isik [32] and Yang [33] reported, the reduction reaction rates of zero-valent iron were first order with respect to the surface area. The heterogeneous reaction of iron-oxide-catalyzed hydrogen peroxide decomposition also follows first order kinetics with respect to the surface area according to Lin and Gurol [23]. Kwan and Voelker [34] revealed that the rates of hydroxyl radical generation in Fenton-like systems catalyzed by different synthesized iron oxides (including ferrihydrite, goethite, or hematite) were all proportional to the surface area of respective iron oxides. Gregor et al [35] prepared crystalline iron oxide (α-Fe_2O_3 and γ-Fe_2O_3) nanoparticles with varied specific surface areas under different thermal treatments, and found that their catalytic efficiencies in hydrogen peroxide decomposition also increased monotonically with increasing specific surface area.

By comparing the surface-area-normalized redox activities of iron nanostructures with different sizes, many studies have found that size-dependent physicochemical surface properties also play an important role in the redox reactions of iron nanostructures. Wang and Zhang [36] found that surface-area-normalized reduction rate constants of zero-valent iron nanoparticles with specific surface area of 33.5 m^2/g were calculated to be 10–100 times higher than those of microparticles with specific surface area of 0.9 m^2/g. As reported by Anschutz and Penn [37], surface-area-normalized reduction dissolution rates for nanoparticles of 4 nm ferrihydrite and 5 nm × 64 nm goethite by hydroquinone are up to 20 times and two times faster than the rates for nanoparticles of 6 nm ferrihydrite and 22 nm × 367 nm goethite, respectively [37]. Cwiertny et al [38] demonstrated that the surface-area-normalized rate of oxalate-promoted dissolution of goethite was four times greater in nanorod suspensions than in microrod suspensions [38]. Similarly, after surface area normalization, the initial and steady state reductive dissolution rates for hematite nanoparticles with average sizes of 6.8 nm by ascorbic acid were about two times and one point five times of those with average size of 30.5 nm according to Echigo et al [39]. The surface physicochemical properties of smaller iron oxide particles thus seem to favor iron dissolution, so that more rapid induction of homogeneous redox reactions could be expected for iron oxide with smaller dimensions. Additionally, specific size-dependent physicochemical surface properties of iron oxides have also been reported. According to Cornell and Schwertmann [40], particle size has a marked effect on the solubilities of iron oxides, due to the relatively high surface free energy of the compounds, and the solubility products (K_{sp}) of hematite and goethite could increase by two orders of magnitude when particle size decreases from 1 μm to 10 nm, as illustrated first by Langmuir [41] in 1971. Chernyshova et al [42] observed a regular increase in tetrahedral defects in the near surface regions of hematite with decreasing particle size, whereas surface defects were well recognized to affect reactivity of metal oxides. Gilbert et al [43] found that surface oxygen sites of 6 nm goethite nanoparticles are less coordinated by iron relative to bulk goethite, and proposed that this could consequently result in the increased redox reactivity of goethite nanoparticles.

3.3. *Crystalline phase*

Iron oxides have a wide range of phases such as ferrihydrite, lepidocrocite, maghemite, goethite, and hematite, and these different phases possess varied abilities to initiate homogeneous and heterogeneous ROS-related redox reactions. To better understand their capacities to induce homogeneous redox reactions, the crystalline-phase-dependent heterogeneous process of iron dissolution should also be considered. The solubility of ferric oxides with sizes above 11 nm at room temperature generally follows the reversed order of thermodynamic stabilities of the crystalline phases, i.e., ferrihydrite > lepidocrocite > maghemite > goethite > hematite [40,44–46], and the iron dissolution rate of these minerals with similar dimensions also seems to follow the same order. Larsena and Postma [47] reported that the surface-area-normalized reduction dissolution rates of ferrihydrite, lepidocrocite, and goethite particles with similar size by ascorbic acid follow the order of ferrihydrite > lepidocrocite > goethite. Roden [48] demonstrated that the surface-area-normalized biological reduction dissolution rate of goethite particles by *Shewanella putrefaciens* strain CN32 was larger than that of hematite with a similar size [48]. According to Bosch et al [49], the surface-area-normalized microbial reduction rate of colloidal goethite and hematite with similar surface areas by *Geobacter sulfurreducens* followed the order of goethite > hematite. Shi et al [50] demonstrated that poorly crystalline 2-line ferrihydrite yielded the highest surface-area-normalized reduction dissolution rate, followed by more crystalline 6-line ferrihydrite and crystalline lepidocrocite with similar size at the nanoscale in the presence of reduced flavin mononucleotide, riboflavin, and anthraquinone-2,6-disulfonate [50]. In 2013, Wang et al [51] detected more dissolved iron in the solutions of maghemite nanoparticles than in the solutions of hematite nanoparticles with similar size at pH 1.2 and pH 4.2, with or without the presence of cysteine and nicotinamide adenine dinucleotide (NADH). In fact, when the dimension is fixed, iron oxides with less thermodynamic stability usually possess higher Gibbs free energies, so their free energy barriers for iron dissolution are lower, which might explain their higher iron dissolution rates.

The heterogeneous Fenton-like redox reactivity of ferric oxides appears to follow the order of thermodynamic stabilities of the crystalline phases. Lee et al [52] prepared ferric oxides with different crystallinity degrees at various calcination temperatures, and found that the surface-area-normalized rates of these compounds in hydrogen peroxide decomposition followed the order of their crystallinity degrees. Hermanek et al [53] demonstrated that increasing crystallinity from amorphous Fe_2O_3 to α-Fe_2O_3 enhanced heterogeneous catalytic efficiencies of the compounds in hydrogen peroxide decomposition. As demonstrated by Wang et al. [51], maghemite nanoparticles showed lower hydroxyl radical generation efficiency in the heterogeneous Fenton-like reactions than did hematite nanoparticles with similar size, which was elucidated by the lower iron oxidation state on the surface of hematite nanoparticles. To date, however, there is still incomplete knowledge about how different crystalline phases influence the redox reactivity of iron oxide nanoparticles.

4. ROS-related bio-microenvironmental factors

During their biotransformation in living organisms, nanomaterials might encounter a wide range of bio-microenvironments, including both extracellular and intracellular biological fluids. Nanomaterials can be adsorbed on the skin, inhaled into the lung, ingested into the gastrointestinal tract, or injected into the blood, and then be internalized into cells of specific tissues through various endocytosis pathways. Within cells, many nanoparticles could end up in the lysosomes, but some of them that are capable of escaping from endosomes or lysosomes might appear in cytoplasm and other cellular organelles such as the Golgi body, mitochondria, and nucleus [54]. The ROS levels in animal blood have been recognized to rise under certain

physiological conditions, such as breeding, hypertension, and inflammation [55]. Within cells, ROS are continuously produced mainly as by-products of electron transportation in the mitochondria, and may also appear in other cellular locations after escaping the effective antioxidant defense [2]. Therefore, in order to understand the biological effects of iron nanostructures, it is crucial to characterize ROS-related activities of nano-iron metal and nano-iron oxides under these bio-microenvironmental conditions.

4.1. *Physiological pH and buffers*

The physiological pH of extracellular and intracellular fluids varies greatly with specific tissues and cellular organelles, and it covers a wide range from acidic to weakly alkaline. The human skin surface maintains a weakly acid physiological pH of about 5.5, whereas the physiological pH of human blood is tightly controlled within a narrow weakly alkaline range of 7.35–7.45. The intravesicular pH value drops along with the endocytic process, from pH 6.0–6.5 in early endosomes to pH 4.5–5.5 in late endosomes and lysosomes [56]. The mitochondrial matrix pH is in the range of 7.7–8.2, about 1 pH unit more alkaline than the cytosolic pH, which is close to 7 [57], whereas Golgi luminal pH values range from 5.95 to 6.45, about 1 pH unit lower than the cytosolic pH [58]. The species of oxidants generated in the redox reactions of ROS and iron nanostructures are greatly influenced by pH, due to the pH-dependent partitioning of radical and non-radical Fenton reactions. Hydroxyl radicals have been well recognized as the dominant oxidants generated at a lower pH, whereas near neutral or alkaline conditions seem to favor the production of ferryl-oxo complexes. Hydroxyl radicals are much more powerful one-electron oxidants than ferryl-oxo complexes, whereas ferryl-oxo complexes can act as both one-electron and two-electron oxidants [15–18]. Distinct substrates and oxidative products can thus be expected in different bio-microenvironments with varying pH values. In 2013, Bataineh et al [16] reported the pH-induced mechanistic changeover from hydroxyl radicals to ferryl-oxo complexes in the homogeneous Fenton reaction, which resulted in the changeover of dimethyl sulfoxide oxidative products from ethane and methane to dimethyl sulfone. According to Lee et al [59], aromatic compounds, i.e., phenol and benzoic acid, were not oxidized by ferryl-oxo complexes generated in homogeneous Fenton reactions under neutral or alkaline pH conditions, unlike methanol, Reactive Black 5, and arsenite, which were oxidized to a different degree depending on the catalytic pH. The physiological pH might also affect the catalytic efficiency of iron nanostructures in hydrogen peroxide decomposition. Lin and Gurol [23] reported that the rate constant of goethite in hydrogen peroxide decomposition increased from 0.019 M^{-1} s^{-1} to 0.067 M^{-1} s^{-1} as pH increased from 5 to 10 [23]. Watts et al [24] revealed that the efficiency of goethite in hydrogen peroxide decomposition increased as a function of pH in the pH range of 4–7 with ferryl-oxo complexes as the dominant oxidant at a higher pH. In 2012, Chen et al [31] reported that magnetite and maghemite nanoparticles exhibited peroxidase-like and catalase-like activities under acidic lysosome and neutral cytosol mimic conditions, respectively (Fig. 1).

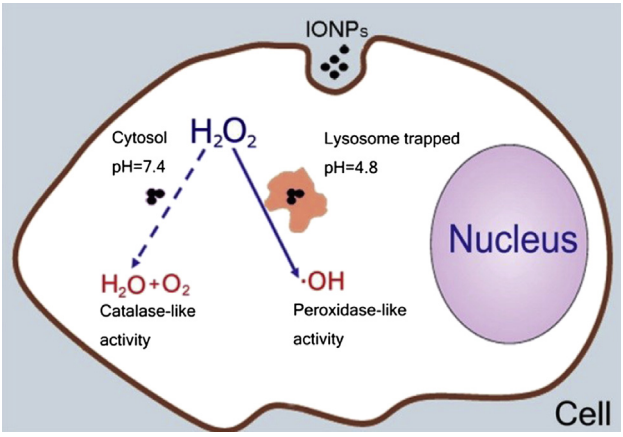

Fig. 1 – Schematic illustration of peroxidase-like activity-induced cytotoxicity by iron oxide nanoparticles (IONPs). IONPs are trapped in acidic lysosomes when internalized into cells, so they catalyze decomposition of H_2O_2 to produce hydroxyl radicals through peroxidase-like activity; however, in neutral cytosol, IONPs would decompose H_2O_2 through catalase-like activity. *Note.* From "Dual enzyme-like activities of iron oxide nanoparticles and their implication for diminishing cytotoxicity," by Z. Chen, J.J. Yin, Y.T. Zhou, et al, 2012, *ACS Nano*, 6, p. 4001–12. Copyright 2012, *ACS Publications*. Reprinted with permission.

Physiological buffering systems help the biological fluids maintain a nearly constant pH, and two important biological buffer systems are the carbonate system and the phosphate system. The carbonate buffering system plays an important role in maintaining the pH of blood plasma, whereas the phosphate buffering system operates in the intracellular biological fluids. Both of these buffering systems have been reported to influence the ROS-related redox activities of iron oxides. Miller and Valentine [60] reported that phosphate could increase the oxidative degradation of quinoline by hydrogen peroxide in the presence of iron oxide, despite its retarding effect on the rate of hydrogen peroxide decomposition catalyzed by iron oxide. Valentine and Wang [61] demonstrated that the oxidant yields of hydrogen peroxide in the presence of iron oxides were increased by the addition of phosphate in the system. Watts et al [24] revealed that phosphate-stabilized hydrogen peroxide exposed to iron oxides carried a higher rate of hydroxyl radical production than did the unstabilized system, in spite of the lower hydrogen peroxide decomposition rates in the stabilized systems [24]. Phosphate also seemingly increases partitioning of the radical mechanism in homogeneous Fenton systems at higher pH levels by retarding non-radical reactions [16]. According to Hug and Leupin [62], bicarbonate could also increase oxidant yield of hydrogen peroxide in the homogeneous Fenton system. Therefore, it is reasonable to postulate that phosphate and carbonate physiological buffering systems could modify the redox properties of iron nanostructures, which might be partly attributed to the modified Fe(II) oxygenation rate constants in the presence of phosphate and carbonate anions, as shown in Table 1 [18,63]. According to the published rate

Table 1 – Fe(II) reaction rates with molecular oxygen and hydrogen peroxide at 25°C.

Species	log k	
	O_2 [a]	H_2O_2 [b]
Fe^{2+}	−6.03 [c]	1.92 [c]
$FeCl^+$	−4.8 [c]	2.1 [c]
$FeSO_4$	−4.8 [c]	2.1 [c]
$Fe(OH)^+$	0.84 [c]	5.58 [c]
$Fe(OH)_2$	5.94 [c]	9.0 [c]
$FeHCO_3$	<0.1 [c]	3.79 [c]
$FeCO_3$	<−0.4 [c]	4.34 [c]
$Fe(CO_3)_2^{2-}$	−4.04 [c]	7.52 [c]
$Fe(CO_3)(OH)^-$	−2.2 [c]	
$FeH_2PO_4^+$	−1.5 [d]	
$FeHPO_4$	−0.91 [d]	
$FePO_4^-$	1.3 [d]	

[a] $M^{-1}\,s^{-1}$, reaction with O_2 to produce $O_2^{-\bullet}$.
[b] $M^{-1}\,s^{-1}$, reaction with H_2O_2 to produce $^\bullet OH$.
[c] In pure water, from [18].
[d] $I = 0.1$, from [63].

constants, oxygenation of Fe(II)-phosphate species ($FeH_2PO_4^+$, $FeHPO_4$, $FePO_4^-$) and Fe(II)-carbonate species [$FeHCO_3$, $FeCO_3$, $Fe(CO_3)_2^{2-}$, $Fe(CO_3)(OH)^-$] is more difficult compared to non-buffered Fe(II)-hydroxy species [$Fe(OH)^+$, $Fe(OH)_2$], so both oxidant-generating and auto-scavenging steps, including reactions of (1), (2), (5–7), (10), (11), (13), and (15–17), in the presence of phosphate and carbonate buffering compounds, could be delayed, which might explain the retardation of hydrogen peroxide decomposition in the buffered systems. Particularly, the efficient hydroxyl radical scavenging activities of phosphate and carbonate could also contribute to a delayed auto-scavenging step, together with the delayed oxygenation of ferrous iron species, and this would result in more oxidants consumed by the substrates [64].

4.2. *Biogenic reducing agents*

Body fluid maintains a reducing environment compared to iron oxides, and various biogenic reducing agents (e.g., glutathione, cysteine, ascorbic acid, NADH, NADPH, succinate, and ubiquinol) with a wide range of E^0 are distributed in extracellular and intracellular biological fluids. Human plasma maintains a mean E^0 of as low as −140 mV, but is still 90 mV more oxidized than the cytoplasmic pool. Among the cellular organelles, the mitochondrion is the most reducing cellular compartment with an E^0 of about −318 mV, followed by lysosome (−240 mV), and endoplasmic reticulum (−189 mV) [65]. It is thus of great biological importance to consider the redox activities of iron nanostructures under reducing bio-microenvironmental conditions.

Reductive dissolution of iron oxide nanoparticles will inevitably induce more homogeneous Fenton reactions, which are much more efficient in producing damaging ROS than heterogeneous Fenton reactions (Fig. 2). Wang et al [51] revealed that significantly larger dissolved iron fractions were detected in solutions containing maghemite and hematite nanoparticles in the presence of cysteine and NADPH under all pH regimes, and they also observed that these fractions induced much more hydroxyl radicals from hydrogen peroxide than the solid surfaces. Substantial evidence also indicates that superparamagnetic iron oxide nanoparticles are gradually degraded in endosomes and lysosomes, where the dissolved iron species cause oxidative stress to induce severe membrane permeation and subsequent cellular dysfunction [66–68].

4.3. *Other organic substances*

In addition to those which function as reducing agents, a wide range of organic substances with diverse biological functionalities and chemical groups (such as carboxylate, phenolate, hydroxy, thiol, and amines) are also ubiquitous in biological fluids. The interactions of these organic substances with homogeneous or heterogeneous iron species can also influence the redox activities of iron nanostructures. According to Lipczynska-Kochany et al [64], anions including the above-mentioned phosphate and carbonate might influence hydrogen peroxide decomposition and oxidant generation through modifying the Fe(II) oxygenation rate and competitive scavenging of reactive intermediates. As demonstrated by Valentine and Wang [61], Fukushima and Tatsumi [69], and Vione et al [70], humic acid could increase oxidant generation efficiencies of homogeneous or heterogeneous Fenton and Fenton-like systems through their carboxyl and phenolate groups. Kachur et al [19] found that hydroxyl radical formation during Fe(II) autoxidation was enhanced significantly by the addition of polyphosphates (tri- and tetrapolyphosphate and their adenosine derivatives), citrate, and acetic derivatives of EDTA, diethylenetriaminepentaacetic acid, triethylenetetraminehexaacetic acid, ethylenediamine-(N,N′)-diacetic acid, and nitrilotriacetic acid (NTA) with the generation rate of hydroxyl radicals showing an inverse correlation with the charge of the ferrous ion complex. Iwahashi et al [71] revealed that a series of organic acids, including quinolinic acid, α-picolinic acid, fusaric acid, and 2,6-pyridinedicarboxylic acid, could enhance the hydroxyl radical yield of the homogeneous Fenton system via Fe(II) chelation. According to Keenan and Sedlak [17], the addition of oxalate, NTA, and EDTA to oxygen-containing solutions of zero-valent iron nanoparticles significantly increased oxidant generation efficiencies, with yields approaching their theoretical maxima near neutral pH. Rey et al [21] reported that phenol could also lead to a higher hydroxyl radical yield in a heterogeneous Fenton-like system, whereas Minakata et al [72] revealed that polyphenols including α-picolinic acid, 2,6-pyridinedicarboxylic acid, and quinolinic acid (2,3-pyridinedicarboxylic acid) enhanced the formation of radicals in the Fenton-like reaction mixture of rat liver microsomes. In addition, Fe(II) organic complexation seems to exert influence on the partitioning of radical and non-radical Fenton mechanisms at neutral pH [17]. Organic substances in the biological fluids can also enhance iron dissolution via ligand-promotion or Fe(II) complexion, therefore more homogeneous ROS-related redox reactions would also be expected in the bio-microenvironments. Duckworth and Martin [73] revealed that C_1–C_6 dicarboxylic acids, including succinate, adipate, oxalate, malonate, and glutarate, enhanced iron dissolution of hematite by forming monodentate or bidentate surface complexation structures, with

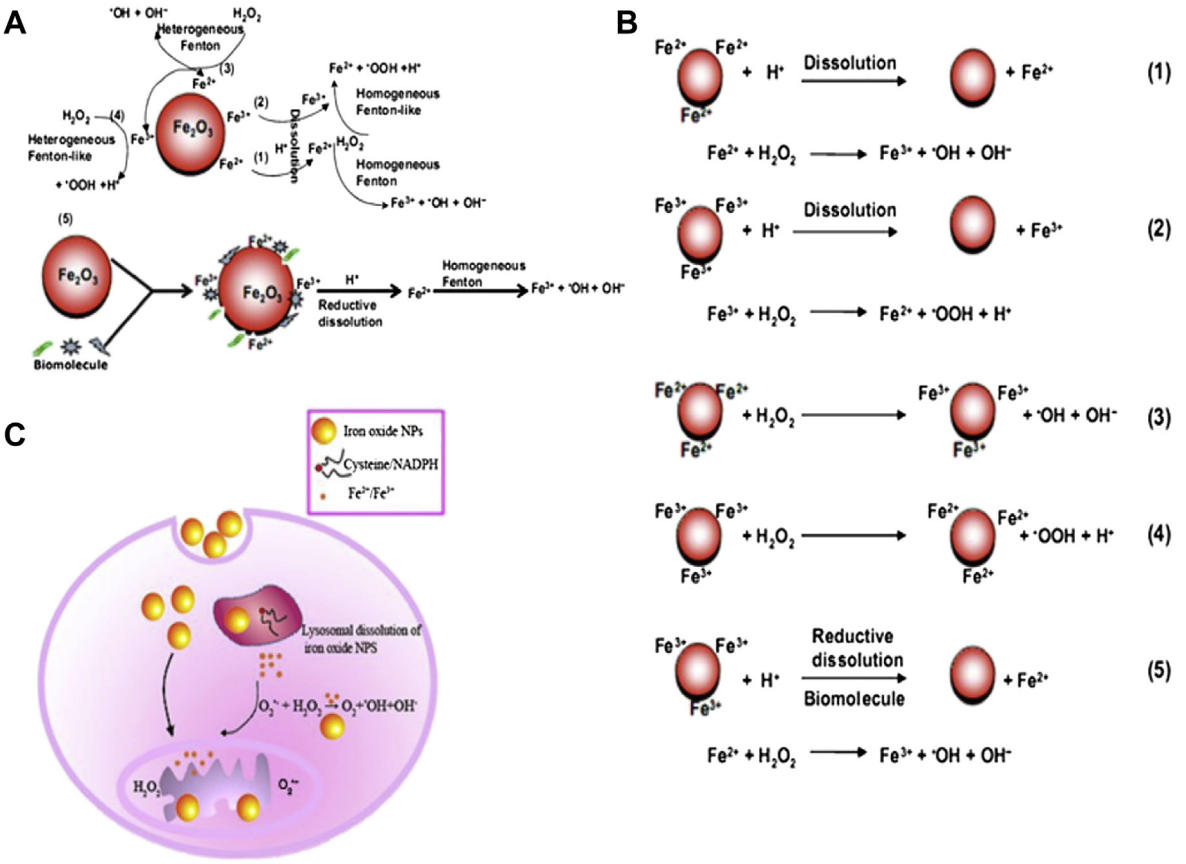

Fig. 2 – Scheme for ·OH free radical generation by iron oxide nanoparticles (NPs) in bio-microenvironments. (A) ·OH generation at the nanobio interface of Fe_2O_3 NPs; (B) chemical processes of ·OH generation by Fe_2O_3 NPs; (C) intracellular ·OH free radical generation: dissolution or *in situ* reductive dissolution of magnetic iron oxide NPs may occur in the acidic lysosomal microenvironment, which depends on surface hydroxylation and surface Fe oxidation state of iron oxide NPs; the free Fe ions or NPs can react with hydrogen peroxide and superoxide in mitochondria and cytoplasm to produce highly reactive ·OH via homogeneous or heterogeneous Fe(II)/Fe(III) catalytic Fenton/Haber-Weiss type reaction. *Note*. From "Physicochemical origin for free radical generation of iron oxide nanoparticles in biomicroenvironment: catalytic activities mediated by surface chemical states," by B. Wang, J.J. Yin, X.Y. Zhou, et al, 2013, *J Phys Chem C*, 117, p. 383–92. Copyright 2012, *ACS Publications*. Reprinted with permission.

bidentate structures more being effective. Royer et al [74] reported that natural organic matter could enhance reductive dissolution of hematite by Fe(II) complexation, which prevents Fe(II) resorption to hematite surfaces.

5. Conclusions and perspectives

In this review, the known ROS-related redox mechanisms of nano-iron metal and nano-iron oxides, including homogeneous and heterogeneous reactions, were discussed in detail. We also provide a general overview on the intrinsic ROS-related properties of these iron nanostructures including chemical composition, particle size, and crystalline phase, which determine the basic redox activities of these compounds. Extrinsic bio-microenvironmental factors, such as physiological pH and buffers, biogenic reducing agents, and other organic substances were also explored because of their potential crucial impact on the biological effects of iron nanostructures. In spite of the large number of studies on iron nanostructures, much remains unknown about how their intrinsic physicochemical properties affect the redox reactivity of iron nanostructures. In particular, additional work is needed to characterize the redox activities of iron nanostructures under various bio-microenvironmental conditions.

Conflicts of interest

All authors declare no conflicts of interest.

Acknowledgments

The financial support of the China Scholarship Council (CSC; No. 201306330015) is gratefully acknowledged.

REFERENCES

[1] Pantopoulos K, Schipper HM. Principles of free radical biomedicine. New York: Nova Science Publisher; 2011.
[2] Ray PD, Huang BW, Tsuji Y. Reactive oxygen species (ROS) homeostasis and redox regulation in cellular signaling. Cell Signal 2012;24:981–90.
[3] Chuankrerkkul N, Sangsuk S. Current status of nanotechnology consumer products and nano-safety issues. J Met Mat Min 2008;18:75–9.
[4] Kessler R. Engineered nanoparticles in consumer products: understanding a new ingredient. Environ Health Perspect 2011;119:A120–5.
[5] Nel A, Xia T, Mädler L, et al. Toxic potential of materials at the nanolevel. Science 2006;311:622–7.
[6] Hadjipanayis CG, Bonder MJ, Balakrishnan S, et al. Metallic iron nanoparticles for MRI contrast enhancement and local hyperthermia. Small 2008;4:1925–9.
[7] Nikonov IN, Folmanis YG, Folmanis GE, et al. Iron nanoparticles as a food additive for poultry. Dokl Biol Sci 2011;440:328–31.
[8] Zhang W. Nanoscale iron particles for environmental remediation: an overview. J Nanopart Res 2003;5:323–32.
[9] Nurmi JT, Tratnyek PG, Sarathy V, et al. Characterization and properties of metallic iron nanoparticles: spectroscopy, electrochemistry, and kinetics. Environ Sci Technol 2005;39:1221–30.
[10] De Caro D, Ely TO, Mari A, et al. Synthesis, characterization, and magnetic studies of nonagglomerated zerovalent iron particles. Unexpected size dependence of the structure. Chem Mater 1996;8:1987–91.
[11] Roghayyeh S, Mohammad S, Shishevan MT, et al. Effects of nano-iron oxide particles on agronomic traits of soybean. Not Sci Biol 2010;2:112–3.
[12] Guo H, Barnard AS. Naturally occurring iron oxide nanoparticles: morphology, surface chemistry and environmental stability. J Mater Chem A 2013;1:27–42.
[13] Haynes WMCRC. Handbook of chemistry and physics. 94th ed. New York: Taylor & Francis; 2013.
[14] Wood PM. The potential diagram for oxygen at pH 7. Biochem J 1988;253:287–9.
[15] Koppenol WH, Liebman JF. The oxidizing nature of the hydroxyl radical. A comparison with the ferryl ion (FeO^{2+}). J Phys Chem 1984;88:99–101.
[16] Bataineh H, Pestovsky O, Bakac A. pH-induced mechanistic changeover from hydroxyl radicals to iron(IV) in the Fenton reaction. Chem Sci 2012;3:1594–9.
[17] Keenan CR, Sedlak DL. Ligand-enhanced reactive oxidant generation by nanoparticulate zero-valent iron and oxygen. Environ Sci Technol 2008;42:6936–41.
[18] King DW, Farlow R. Role of carbonate speciation on the oxidation of Fe(II) by H_2O_2. Mar Chem 2000;70:201–9.
[19] Kachur AV, Tuttle SW, Biaglow JE. Autoxidation of ferrous ion complexes: a method for the generation of hydroxyl radicals. Radiat Res 1998;150:475–82.
[20] Mizutani Y, Hashimoto S, Tatsuno Y, et al. Resonance Raman pursuit of the change from iron(II)-oxygen (FeII-O_2) to iron(III)-hydrohxyl (FeIII-OH) via iron(IV):oxygen (FeIV: O) in the autoxidation of ferrous iron-porphyrin. J Am Chem Soc 1990;112:6809–14.
[21] Rey A, Bahamonde A, Casas JA, et al. Selectivity of hydrogen peroxide decomposition towards hydroxyl radicals in catalytic wet peroxide oxidation (CWPO) over Fe/AC catalysts. Water Sci Technol 2010;61:2769–78.
[22] Zalma R, Bonneau L, Guignard J, et al. Production of hydroxyl radicals by iron solid compounds. Toxicol Environ Chem 1987;13:171–87.
[23] Lin SS, Gurol MD. Catalytic decomposition of hydrogen peroxide on iron oxide: kinetics, mechanism, and implications. Environ Sci Technol 1998;32:1417–23.
[24] Watts RJ, Foget MK, Kong S, et al. Hydrogen peroxide decomposition in model subsurface systems. J Hazard Mater 1999;69:229–43.
[25] Pham AL, Lee C, Doyle FM, et al. A silica-supported iron oxide catalyst capable of activating hydrogen peroxide at neutral pH values. Environ Sci Technol 2009;43:8930–5.
[26] Fang GD, Zhou DM, Dionysiou DD. Superoxide mediated production of hydroxyl radicals by magnetite nanoparticles: demonstration in the degradation of 2-chlorobiphenyl. J Hazard Mater 2013;250–251:68–75.
[27] Keenan CR, Sedlak DL. Factors affecting the yield of oxidants from the reaction of nanoparticulate zero-valent iron and oxygen. Environ Sci Technol 2008;42:1262–7.
[28] Xue X, Hanna K, Deng N. Fenton-like oxidation of Rhodamine B in the presence of two types of iron (II, III) oxide. J Hazard Mater 2009;166:407–14.
[29] Gorski CA, Nurmi JT, Tratnyek PG, et al. Redox behavior of magnetite: implications for contaminant reduction. Environ Sci Technol 2010;44:55–60.
[30] Voinov MA, Sosa Pagán JO, Morrison E, et al. Surface-mediated production of hydroxyl radicals as a mechanism of iron oxide nanoparticle biotoxicity. J Am Chem Soc 2011;133:35–41.
[31] Chen Z, Yin JJ, Zhou YT, et al. Dual enzyme-like activities of iron oxide nanoparticles and their implication for diminishing cytotoxicity. ACS Nano 2012;6:4001–12.
[32] Sponza DT, Isik M. Decolorization and azo dye degradation by anaerobic/aerobic sequential process. Enzyme Microb Technol 2002;31:102–10.
[33] Yang H. Zero-valent iron decolorization of the anthraquinone dye Reactive Blue 4 and biodegradation assessment of its decolorization products. Thesis. Georgia Institute of Technology; 2005. p. 61–95.
[34] Kwan WP, Voelker BM. Rates of hydroxyl radical generation and organic compound oxidation in mineral-catalyzed Fenton-like systems. Environ Sci Technol 2003;37:1150–8.
[35] Gregor C, Hermanek M, Jancik D, et al. The effect of surface area and crystal structure on the catalytic efficiency of iron(III) oxide nanoparticles in hydrogen peroxide decomposition. Eur J Inorg Chem 2010;2010:2343–51.
[36] Wang CB, Zhang W. Synthesizing nanoscale iron particles for rapid and complete dechlorination of TCE and PCBs. Environ Sci Technol 1997;31:2154–6.
[37] Anschutz AJ, Penn RL. Reduction of crystalline iron(III) oxyhydroxides using hydroquinone: influence of phase and particle size. Geochem Trans 2005;6:60–6.
[38] Cwiertny DM, Hunter GJ, Pettibone JM, et al. Surface chemistry and dissolution of α-FeOOH nanorods and microrods: Environmental implications of size-dependent interactions with oxalate. J Phys Chem C 2009;113:2175–86.
[39] Echigo T, Aruguete D, Murayama M, et al. Influence of size, morphology, surface structure, and aggregation state on reductive dissolution of hematite nanoparticles with ascorbic acid. Geochim Cosmochim Ac 2009;90:149–62.
[40] Cornell RM, Schwertmann U. The iron oxides: structure, properties, reactions, occurrences and uses. 2nd ed. New York: John Wiley & Sons; 2003.
[41] Langmuir D. Particle size effect on the reaction goethite = hematite + water. Am J Sci 1971;271:147–56.
[42] Chernyshova IV, Hochella MF, Madden AS. Size-dependent structural transformations of hematite nanoparticles. 1. Phase transition. Phys Chem Chem Phys 2007;9:1736–50.

[43] Gilbert B, Kim CS, Dong CL, et al. Oxygen K-edge emission and absorption spectroscopy of iron oxyhydroxide nanoparticles. AIP Conf Proc 2007;882:721–5.
[44] Navrotsky A, Mazeina L, Majzlan J. Size-driven structural and thermodynamic complexity in iron oxides. Science 2008;319:1635–8.
[45] Guo H, Barnard AS. Thermodynamic modelling of nanomorphologies of hematite and goethite. J Mater Chem 2011;21:11566–77.
[46] Schwertmann U. Solubility and dissolution of iron oxides. Plant Soil 1991;130:1–25.
[47] Larsena O, Postma D. Kinetics of reductive bulk dissolution of lepidocrocite, ferrihydrite, and goethite. Geochim Cosmochim Ac 2001;65:1367–79.
[48] Roden EE. Fe(III) oxide reactivity toward biological versus chemical reduction. Environ Sci Technol 2003;37:1319–24.
[49] Bosch J, Heister K, Hofmann T, et al. Nanosized iron oxide colloids strongly enhance microbial iron reduction. Appl Environ Microbiol 2010;76:184–9.
[50] Shi Z, Zachara JM, Shi L, et al. Redox reactions of reduced flavin mononucleotide (FMN), riboflavin (RBF), and anthraquinone-2,6-disulfonate (AQDS) with ferrihydrite and lepidocrocite. Environ Sci Technol 2012;46:11644–52.
[51] Wang B, Yin JJ, Zhou XY, et al. Physicochemical origin for free radical generation of iron oxide nanoparticles in biomicroenvironment: catalytic activities mediated by surface chemical states. J Phys Chem C 2013;117:383–92.
[52] Lee S, Oh J, Park Y. Degradation of phenol with Fenton-like treatment by using heterogeneous catalyst (modified iron oxide) and hydrogen peroxide. Bull Korean Chem Soc 2006;27:489–94.
[53] Hermanek M, Zboril R, Medrik I, et al. Catalytic efficiency of iron(III) oxides in decomposition of hydrogen peroxide: competition between the surface area and crystallinity of nanoparticles. J Am Chem Soc 2007;129:10929–36.
[54] Zhao Yuliang, Wang Bing, Feng Weiyue, Bai Chunli. Nanotoxicology: toxicological and biological activities of nanomaterials. In: Encyclopedia of Life Support Systems (EOLSS): nanoscience and nanotechnologies. Paris: UNESCO-EOLSS Publishers; 2010.
[55] Hartono SP, Knudsen BE, Zubair AS, et al. Redox signaling is an early event in the pathogenesis of renovascular hypertension. Int J Mol Sci 2013;14:18640–56.
[56] Sorkin A, Von Zastrow M. Signal transduction and endocytosis: close encounters of many kinds. Nat Rev Mol Cell Biol 2002;3:600–14.
[57] Akhmedov D, Braun M, Mataki C, et al. Mitochondrial matrix pH controls oxidative phosphorylation and metabolism-secretion coupling in INS-1E clonal beta cells. FASEB J 2010;24:4613–26.
[58] Thompson RJ, Nordeen MH, Howell KE, et al. A large-conductance anion channel of the Golgi complex. Biophys J 2002;83:278–89.
[59] Lee H, Lee HJ, Sedlak DL, Lee C. pH-Dependent reactivity of oxidants formed by iron and copper-catalyzed decomposition of hydrogen peroxide. Chemosphere 2013;92:652–8.
[60] Miller CM, Valentine RL. Hydrogen peroxide decomposition and quinoline degradation in the presence of aquifer material. Water Res 1995;29:2353–9.
[61] Valentine RL, Wang HCA. Iron oxide surface catalyzed oxidation by quinoline by hydrogen peroxide. J Environ Eng 1998;124:31–8.
[62] Hug SJ, Leupin O. Iron-catalyzed oxidation of arsenic(III) by oxygen and by hydrogen peroxide: pH-dependent formation of oxidants in the Fenton reaction. Environ Sci Technol 2003;37:2734–42.
[63] MaoY Pham ANP, Rose AL, et al. Influence of phosphate on the oxidation kinetics of nanomolar Fe(II) in aqueous solution at circumneutral pH. Geochim Cosmochim Ac 2011;75:4601–10.
[64] Lipczynska-Kochany E, Sprah G, Harms S. Influence of some groundwater and surface waters constituents on the degradation of 4-chlorophenol by the Fenton reaction. Chemosphere 1995;30:9–20.
[65] Go YM, Jones DP. Redox compartmentalization in eukaryotic cells. Biochim Biophys Acta 2008;1780:1273–90.
[66] Arbab AS, Wilson LB, Ashari P, et al. A model of lysosomal metabolism of dextran coated superparamagnetic iron oxide (SPIO) nanoparticles: implications for cellular magnetic resonance imaging. NMR Biomed 2005;18:383–9.
[67] Laskar A, Ghosh M, Khattak SI, et al. Degradation of superparamagnetic iron oxide nanoparticle-induced ferritin by lysosomal cathepsins and related immune response. Nanomedicine (Lond) 2012;7:705–17.
[68] Apopa PL, Qian Y, Shao R, et al. Iron oxide nanoparticles induce human microvascular endothelial cell permeability through reactive oxygen species production and microtubule remodeling. Part Fibre Toxicol 2009;6:1.
[69] Fukushima M, Tatsumi K. Effects of humic substances on the oxidation of pentachlorophenol by peroxosulfate catalyzed by iron(III)-phthalocyanine-tetrasulfonic acid. Bioresour Technol 2006;97:1605–11.
[70] Vione D, Merlo F, Valter M, et al. Effect of humic acids on the Fenton degradation of phenol. Environ Chem Lett 2004;2:129–33.
[71] Iwahashi H, Kawamori H, Fukushima K. Quinolinic acid, α-picolinic acid, fusaric acid, and 2,6-pyridinedicarboxylic acid enhance the Fenton reaction in phosphate buffer. Chem Biol Interact 1999;118:201–15.
[72] Minakata K, Fukushima K, Nakamura M, et al. Effect of some naturally occurring iron ion chelators on the formation of radicals in the reaction mixtures of rat liver microsomes with ADP, Fe^{3+} and NADPH. J Clin Biochem Nutr 2011;49:207–15.
[73] Duckworth OW, Martin ST. Surface complexation and dissolution of hematite by C-1-C-6 dicarboxylic acids at pH 5.0. Geochim Cosmochim Acta 2001;65:4289–301.
[74] Royer RA, Burgos WD, Fisher AS, et al. Enhancement of biological reduction of hematite by electron shuttling and Fe(II) complexation. Environ Sci Technol 2002;36:1939–46.